The effect of carbon dioxide availability on succinic acid production with biofilms of *Actinobacillus succinogenes*

Jolandi Herselman[a], Michael F.A. Bradfield[a], Uma Vijayan[a] & Willie Nicol[a]*

[a]Department of Chemical Engineering, University of Pretoria, Lynnwood Road, Hatfield, 0002, Pretoria, South Africa

Postal address: Department of Chemical Engineering, University of Pretoria, Private Bag X20, Hatfield, 0028, South Africa

Contact details:

Prof. Willie Nicol (corresponding author)*

willie.nicol@up.ac.za | Tel.: +27 12 420 3796 | Fax: +27 12 420 5048

Ms. Jolandi Herselman

herselman.jolandi@gmail.com

Mr. Michael Bradfield

michael.bradfield@tuks.co.za

Ms Uma Vijayan

u10065424@tuks.co.za

Highlights

- Succinic acid productivity starts to decrease with decreasing dissolved CO_2 below an upper threshold
- The decrease in productivity occurs at a constant flux distribution up to a lower CO_2 threshold
- Below the lower threshold, succinic acid yields decrease as flux shifts to C_3 pathways
- Ethanol formation increases with decreasing dissolved CO_2 below the lower threshold

Abstract

Carbon dioxide serves as a co-substrate in succinic acid (SA) production by *Actinobacillus succinogenes* making it an important consideration in fermentation optimisation. In the current study, the availability of CO_2 to the cell, as the dissolved CO_2 concentration in the fermentation broth (C_{CO_2}), is shown to define three distinct steady-state regimes. At C_{CO_2} values between 8.4 mM (±36.8% saturation) and saturation (22.8 mM), there is no evidence of CO_2 limiting SA productivity and flux to SA is constant. As C_{CO_2} is decreased, an upper C_{CO_2} threshold (±36.8% saturation; 8.4 mM) is reached where metabolic flux distributions remain constant but SA productivity and substrate uptake start to decline with decreasing C_{CO_2} levels. A further decrease in C_{CO_2} leads to a lower C_{CO_2} threshold (±17.1% saturation, 3.9 mM) where SA productivity continues to decrease with a concomitant shift in carbon flux away from SA towards C_3 fermentative pathways including ethanol. Since SA production is not limited at relatively low C_{CO_2} values (±36.8% saturation), adequate CO_2 supply to the fermenter can be achieved without requiring major CO_2 sparging schemes which is favourable from an industrial processing perspective.

Keywords: *Actinobacillus succinogenes;* succinic acid; biofilm; CO_2; metabolic flux distribution; mass transfer coefficient

1. Introduction

Succinic acid has been identified as a top value-added [1] and bulk [2] chemical derived from biomass. This stems from both its presence in the tricarboxylic acid cycle which makes biological production plausible, as well as its potential to serve as a substitute and precursor for a number of petrochemicals, thereby augmenting the established market for SA [3]. In addition, SA can be employed as a reagent in the synthesis of bio-polymers such as polybutylene succinate and polyurethane [4]. Although bio-based SA production offers environmental advantages, its successful commercialisation is dependent on cost-competitive production compared to the traditional petrochemical route. To this end, a conversion process is required where a microbial host efficiently converts renewable feedstock into SA.

Various microbial strains have been investigated for SA production with the most promising being *Actinobacillus succinogenes*, *Anaerobiospirillum succiniciproducens, Mannheimia succiniciproducens* and recombinant strains of *Escherichia coli* [5]. Despite competitive performance achieved by all these organisms, *A. succinogenes* has received substantial interest due to its ability to naturally produce SA at appreciable titres, yields and productivities. Furthermore, *A. succinogenes* is tolerant to high acid concentrations [6], is able to convert a variety of carbohydrates to SA [7], and consumes CO_2 in SA synthesis [8].

Given that CO_2 is a co-substrate in the production of succinic acid, the effect of CO_2 supply on SA production was studied in early publications on *A. succinogenes* [7,8]. Diffusion of dissolved CO_2 across the cell membrane is the main transport mechanism for inorganic carbon supply to the cell, since HCO_3^- permeation through the lipid membrane is insignificant [9,10]. Accordingly, the transient concentration of dissolved CO_2 in the broth (C_{CO_2}) is the main driver for CO_2 uptake by the cell. During fermentation, C_{CO_2} will decrease if the rate of CO_2 uptake by the cell exceeds the rate of CO_2 supply to the fermentation broth. CO_2 can

either be supplied as a gas, requiring gas-liquid mass transfer, or in the form of a carbonate (i.e. HCO_3^-, CO_3^{2-}) in the liquid medium. Carbonate salts that are insoluble in water, such as $MgCO_3$ and $CaCO_3$, are often used as a source of CO_2 in fermentation media [8,10,11]. For these cases, the dissolution rate of the solid will be the rate determining step since the carbonate-bicarbonate-CO_2 equilibrium is rapidly established. Under typical fermentation conditions (pH = 6.8, T = 37 °C and CO_2 atmosphere at 1 bar) the dissolved carbonate concentration is low, while bicarbonate and dissolved CO_2 are present at approximately equal concentrations. The highest possible C_{CO_2} value is determined by the CO_2 partial pressure in the gas phase and is in the vicinity of 20 mM for pure CO_2 at atmospheric pressure [10–12].

It has been shown that the supply of CO_2 influences SA productivity and catabolite distribution in *A. succinogenes* fermentations [8,10,11]. All these studies were performed in batch fermentations where the initial carbonate/bicarbonate concentrations and CO_2 partial pressures were varied. Although these studies demonstrate that carbonate supply can have a detrimental effect on the fermentation outcome, the mechanism of the effect is unclear. In the majority of the experiments performed in these studies, only the final cumulative outcome of the batch fermentation is reported. However, the rate of formation of succinic acid varies appreciably within a batch run as there is an initial growth period followed by product inhibition towards the latter stages of the fermentation [6,13]. Accordingly, the uptake rate of CO_2 remains variable throughout the fermentation likely causing fluctuations in C_{CO_2}. In one study [10], the CO_2 supply is shown to be stoichiometrically limited by the initial concentration of carbonates (since carbonates are not replenished during the fermentation), thereby causing a CO_2 shortage before the fermentation is complete. However, as mentioned above only the final, cumulative effect is reported. Variations in CO_2 partial pressure can be used to estimate the value of C_{CO_2} at saturation, although this does not guarantee that the

broth is saturated because gas-liquid mass transfer can be rate controlling leading to C_{CO_2} falling below the saturation value.

Proper design and scale-up of a succinic acid fermentation process cannot rely solely on the results of lab-scale systems. In addition, it is important that the supply of CO_2 be linked to the transient value of C_{CO_2} which drives the inorganic carbon supply. When opting for a gaseous CO_2 supply, gas-liquid mass transfer should be carefully considered in order to achieve adequate C_{CO_2} values without excessive (and expensive) sparging schemes. For carbonate supply, the influence of mixing on the dissolution rate of the solids should be considered in order to maintain the required C_{CO_2} value in the medium. Both these routes require proper understanding and quantification of the effect of C_{CO_2} on succinic acid yield and cell-based productivity. To date, studies have not addressed these crucial relationships but only hint at the importance of CO_2 supply in SA fermentations.

In the current paper, the above mentioned shortcoming in *A. succinogenes* fermentation literature is addressed. Continuous fermentations were performed to enable steady-state analysis of the influence of C_{CO_2} on succinic acid fermentations with *A. succinogenes.* Steady-state conditions ensure that C_{CO_2} remains constant thereby allowing for a more accurate assessment of its influence on yield and cellular productivity. Gas-liquid mass transfer measurements were performed to calculate C_{CO_2} at various steady-state conditions. The amount of immobilised biomass was controlled by operating at glucose-limiting conditions since continuous fermentations with *A. succinogenes* using rich growth media inevitably result in extensive biofilm formation. Mass balances were performed to ensure that all the major metabolites were accounted for.

2. Materials and methods

Organism and fermentation medium

Cultures of *Actinobacillus succinogenes* 130Z (DSM 22257; ATCC 55618), acquired from the German Collection of Microorganisms and Cell Cultures (DSMZ), were maintained in 66% v/v glycerol solutions at -40 °C. Inoculum was prepared in sterilised tryptone soy broth at

30 g L^{-1} and incubated at 37 °C and 150 rpm for 16 to 24 h in 30-mL sealed vials. Prior to inoculation, inoculum was analyzed by HPLC to ensure culture purity and consistent metabolite distributions.

All chemicals were obtained from Merck KgaA unless indicated otherwise. The fermentation medium consisted of three parts: (1) a nutrient and salts mixture, (2) a carbohydrate solution and (3) a phosphate buffer. The nutrient and salts mixture was based on [14] and consisted of (in g L^{-1}): 16.0 yeast extract, 1.0 NaCl, 0.2 $MgCl_2 \cdot 6H_2O$, 0.2 $CaCl_2 \cdot 2H_2O$, sodium acetate (1.36), $Na_2S \cdot 9H_2O$ (0.16) and 0.5 - 1 mL L^{-1} Antifoam Y-30 (Sigma-Aldrich, Germany). The phosphate buffer comprised 1.6 g L^{-1} KH_2PO_4 and 0.8 g L^{-1} K_2HPO_4. Glucose solutions were prepared at 25 g L^{-1}.

Continuous fermentations

Three fermentations were performed in a custom, externally-recycled bioreactor, similar to that used in [15]. The volume was maintained at 358 mL by means of an overflow tube connected to an exit pump. pH was measured by a Ceragel CPS71D glass electrode (Endress+Hauser, Germany) connected to a Liquiline CM442 unit (Endress+Hauser, Germany) and controlled at 6.80 ± 0.01 by the addition of 10 N NaOH. Temperature was measured by the pH electrode and controlled at 37.0 ± 0.1 °C by means of a custom PID feedback controller coupled to a hotplate. A 20% v/v solution of Antifoam Y-30 (Sigma-

Aldrich, Germany) was dosed onto the liquid headspace as needed. The average flow rates of NaOH and antifoam were determined in real-time over a 4-hr period and used to adjust feed concentrations due to dilution of the feed [16]. Furthermore, the time-profile of the average NaOH flow rate was used to estimate steady-state conditions. When the time-averaged dosing was relatively constant, showing only a 10% fluctuation around the average, it was assumed that the system had reached steady-state. CO_2 gas (Afrox, South Africa) served as the inorganic carbon source and was fed directly into the recycle line at different flow rates (i.e. vvm). A vvm of 0.1 was sufficient to ensure CO_2 saturation of the fermentation broth. CO_2 flow rates were controlled using a Brooks 5850S mass flow controller (Brooks Instruments, Hungary). The reactor and liquid reservoirs (excluding NaOH) were autoclaved together at 121 °C for 60 min, with the three parts of the feed medium kept separate to prevent unwanted reactions.

A single wooden stick covered with strands of fiberglass was added to the centre of the reactor body in order to provide additional attachment area and support for biofilm.

Analytical methods

Samples were collected via the outlet pump. The sample container was placed in an ice bath to prevent further metabolic reactions taking place during sampling. The concentrations of glucose, ethanol and organic acids were determined using High-Performance Liquid Chromatography (HPLC). Analyses were performed using an Agilent 1260 Infinity HPLC (Agilent Technologies, USA), equipped with an RI detector and a 300 mm x 7.8 mm Aminex HPX-97 ion-exchange column (Bio-Rad Laboratories, USA). An H_2SO_4 solution was used as the mobile phase at a flowrate of 0.6 $mL.min^{-1}$ with a column temperature of 60 $^{\circ}C$. To overcome co-elution of chromatogram peaks, each sample was analysed with 5-mM and 20-mM mobile phase solutions [15]. In the HPLC system used in the study, the retention time of

acids decreases with increasing mobile phase acidity while the retention time of carbohydrates remains approximately constant, thereby allowing for separation of carbohydrate and acid peaks. Mass balances were performed by comparing the experimental amount of glucose consumed to the stoichiometric amount of glucose required to produce the measured metabolite concentrations [14].

Control at substrate-limiting conditions

At relatively high acid titres (C_{SA} > 10 $g.L^{-1}$) growth of *A. succinogenes* is inhibited but does not terminate completely [17]. Under steady-state conditions of the reactor, it is assumed that limited growth occurs at all times, but cell accumulation is countered by biomass removal. On average these two rates should be similar in order to account for the observed steady-state behaviour (i.e. no net accumulation or removal of cells). However, if residual substrate is present in the broth, a secondary, long-term effect can occur where the biomass content in the fermenter (and the biomass in the outlet) gradually increases over extended periods while pseudo steady-state prevails. This effect needs to be prevented in order to maintain a constant amount of active biomass in the fermenter. To this end, continued cell growth was prevented by operating the reactor under substrate-limiting conditions (i.e. complete glucose conversion).

Overall cellular activity in the reactor is defined as the product of the concentration of active cells and specific cellular activity. Given a constant cellular concentration in the fermenter, if cellular activity decreases, substrate "breakthrough" can occur and the new availability of substrate could allow cellular activity or growth to increase. When substrate breakthrough occurs, the substrate loading needs to be decreased in order to maintain near-complete substrate conversion. To achieve this, the dilution rate can be decreased in proportion to the decrease in cellular activity. Thus, the amount of biomass in the fermenter is maintained and the decrease in dilution rate will directly relate to the decrease in activity. Moreover,

regulating the glucose consumption by decreasing the dilution rate ensures that the total acid concentration remains relatively stable and the inhibitory effect of acids [6] remains constant. Therefore, the true influence of CO_2 availability can be observed without interference from fluctuations in acid titre and cell growth.

Dissolved CO_2 calculations

Mass transfer tests were performed in a liquid solution similar to the fermentation medium but excluded glucose and yeast extract. Mass transfer tests were conducted directly after the first fermentation (Run 1) in order to determine whether the presence of biomass influences mass transfer efficiency. The absence of glucose and yeast extract caused the remaining biomass in the reactor to be metabolically inactive.

In order to calculate the dissolved CO_2 concentration in the fermentation broth, the following three processes need to be considered:

(A) Gas to liquid mass transfer

The volumetric CO_2 mass transfer rate (r_{CO_2}) from the gas bubble to the liquid fermentation broth (bulk liquid), with units of $mol.L^{-1}.h^{-1}$, is given by Eq. (1).

$$-r_{CO_2} = k_g a_g (C^*_{CO_2} - C_{CO_2}) \quad (1)$$

In Eq. (1), $k_g a_g$ is the mass transfer coefficient (h^{-1}), $C^*_{CO_2}$ is the saturated CO_2 concentration at a specific CO_2 partial pressure ($mol.L^{-1}$) and C_{CO_2} is the dissolved CO_2 concentration in the bulk liquid ($mol.L^{-1}$).

(B) Gas-liquid equilibrium

Eq. (2) can be used to calculate the maximum dissolved CO_2 concentration ($mol.L^{-1}$) in the liquid at a known CO_2 partial pressure ($P^*_{CO_2}$) in kPa.

$$C^{*}_{CO_2} = \frac{P^{*}_{CO_2}}{H} \quad (2)$$

H is Henry's constant (kPa.L.mol^{-1}) for CO_2 in a pure solvent. However, since the fermentation medium contains various salts and organic substances, the solubility of CO_2 will be affected and therefore Henry's constant needs to be adjusted accordingly [10–12].

(C) CO_2-carbonate equilibrium.

As CO_2 dissolves in water, the equilibrium reactions given by Eq. (3) to (5) take place under steady-state conditions [10,11]. These reactions occur rapidly and equilibrium is established instantaneously.

$$CO_2 + H_2O \leftrightarrow H_2CO_3 \qquad K_1 = \frac{C^{eq}_{H_2CO_3}}{C^{eq}_{CO_2}} \quad (3)$$

$$H_2CO_3 \leftrightarrow HCO_3^- + H^+ \qquad K_2 = \frac{C^{eq}_{HCO_3^-} C^{eq}_{H^+}}{C^{eq}_{H_2CO_3}} \quad (4)$$

$$HCO_3^- \leftrightarrow H^+ + CO_3^{2-} \qquad K_3 = \frac{C^{eq}_{CO_3^{2-}} C^{eq}_{H^+}}{C^{eq}_{HCO_3^-}} \quad (5)$$

Carbonic acid (H_2CO_3) is highly unstable in solution and is easily broken down. Therefore, Eq. (3) and (4) can be combined to form Eq. (6). Also, at a pH of 6.8, carbonate formation is insignificant and therefore Eq. (5) is not included in the CO_2 transfer model.

$$CO_2 + H_2O \leftrightarrow HCO_3^- + H^+ \qquad K_4 = K_1 \times K_2 = \frac{C^{eq}_{HCO_3^-} C^{eq}_{H^+}}{C^{eq}_{CO_2}} \quad (6)$$

Taking the effects discussed in A, B and C into account, a hydronium ion (Eq. (7)) and inorganic carbon (Eq.(8)) balance was performed for a continuous flow system with continuous CO_2 sparing. No consumption of CO_2 occurred since the biomass was inactive but CO_2 was continuously removed from the system.

Eq. (7) states that the amount of base added is equal to the sum of the hydronium ions formed in the equilibrium reaction (Eq. (6)) and the amount required to increase the pH of the feed from 6.4 to 6.8 (set point).

$$Q_D C_{OH} = \left[\frac{K_4}{C_{H^+}}\right] Q.C_{CO_2} + Q_{feed}(C_{H^+}^{feed} - C_{H^+}) \quad (7)$$

Q_D is the sodium hydroxide flow rate ($L.h^{-1}$), C_{OH} is the concentration of the sodium hydroxide solution ($mol.L^{-1}$), Q is the total flow rate through the reactor ($L.h^{-1}$), Q_{feed} is the feed flow rate into the vessel ($L.h^{-1}$), $C_{H^+}^{feed}$ is the hydronium ion concentration at the feed pH, C_{H^+} is the hydronium ion concentration at the operating pH ($mol.L^{-1}$) and K_4 is the equilibrium constant in Eq. (6).

Eq. (8) states that the amount of CO_2 transferred based on H^+ production from the equilibrium reaction (Eq.(6)) should be equal to the CO_2 mass transfer rate.

$$\left[1+\frac{K_4}{C_{H^+}}\right] QC_{CO_2} = k_g a_g \left(C_{CO_2}^{*} - C_{CO_2}\right) V \quad (8)$$

The value for K_4 in literature is reported as $K_4 = 5.35 \times 10^{-7}$ $mol.L^{-1}$ at 39°C [11]. However, there is a measure of uncertainty regarding the variation of K_4 with temperature and feed composition. The first mass transfer experiments were performed to calculate a unique K_4 value for the system used in the current study. These mass transfer tests were conducted at saturated conditions, i.e. low dilution rates ($D = 0.2\ h^{-1}$) and high CO_2 flow rates (vvm = 15%). During saturated conditions, a decrease in vvm will not significantly decrease the NaOH flow rate. With Q_D measured and all the other parameters of Eq. (7) known, a value for $\frac{K_4}{C_{H^+}}$ could be calculated. $\frac{K_4}{C_{H^+}}$ was found to be equal to 4.45, giving a value of 7.053×10^{-7} $mol.L^{-1}$ for K_4. With K_4 known, further mass transfer tests were carried out in which the CO_2 vvm was varied to determine its effect on the mass transfer coefficient. The second set of

mass transfer tests were performed at a high dilution rate (1.0 h^{-1}) to ensure that C_{CO_2} was sufficiently lower than the saturation point ($C_{CO_2} < 0.7C^*_{CO_2}$). When Q_D and Q at each vvm are known, Eq. (7) and Eq. (8) can be used to solve for $k_g a_g$ and C_{CO_2}.

During fermentation, the effect of CO_2 consumption by the active biomass has to be taken into account. Adding a CO_2 consumption term to Eq. (8) yields Eq. (9) which can be used to calculate the dissolved CO_2 concentration when $k_g a_g$ is known.

$$\left[1+\frac{K_4}{C_{H^+}}\right] QC_{CO_2} = k_g a_g\left(C^*_{CO_2} - C_{CO_2}\right)V - r_{CO_2}V \qquad (9)$$

3. Results and discussion

CO_2 mass transfer under continuous conditions

In investigating the influence of CO_2 availability on succinic acid productivity and yield, it is more appropriate to use a basis that is not specific to reactor geometry but rather more generalised. To this end, the dissolved CO_2 concentration (C_{CO_2}) in the fermentation broth was chosen as the basis and not simply CO_2 flow rate or mass transfer constants (i.e. vvm and $k_g a_g$). To indirectly determine C_{CO_2}, it is first necessary to determine the gas-based mass transfer coefficient, $k_g a_g$. As such, $k_g a_g$ was determined for each steady-state condition across a range of vvm values as described in *Materials and methods*. As can be seen in Fig. 1, $k_g a_g$ increases linearly with increasing vvm indicating that increased CO_2 flow rates contribute directly to improved CO_2 transfer into the fermentation broth and therefore increased availability of CO_2 to the cell.

During the mass transfer experiments, the biomass present in the reactor dissolved and systematically washed out of the reactor after the fermentation medium was replaced with the

Fig. 1. The gas-based CO_2 mass transfer coefficient ($k_g a_g$) as a function of CO_2 gas flow rate (wm).

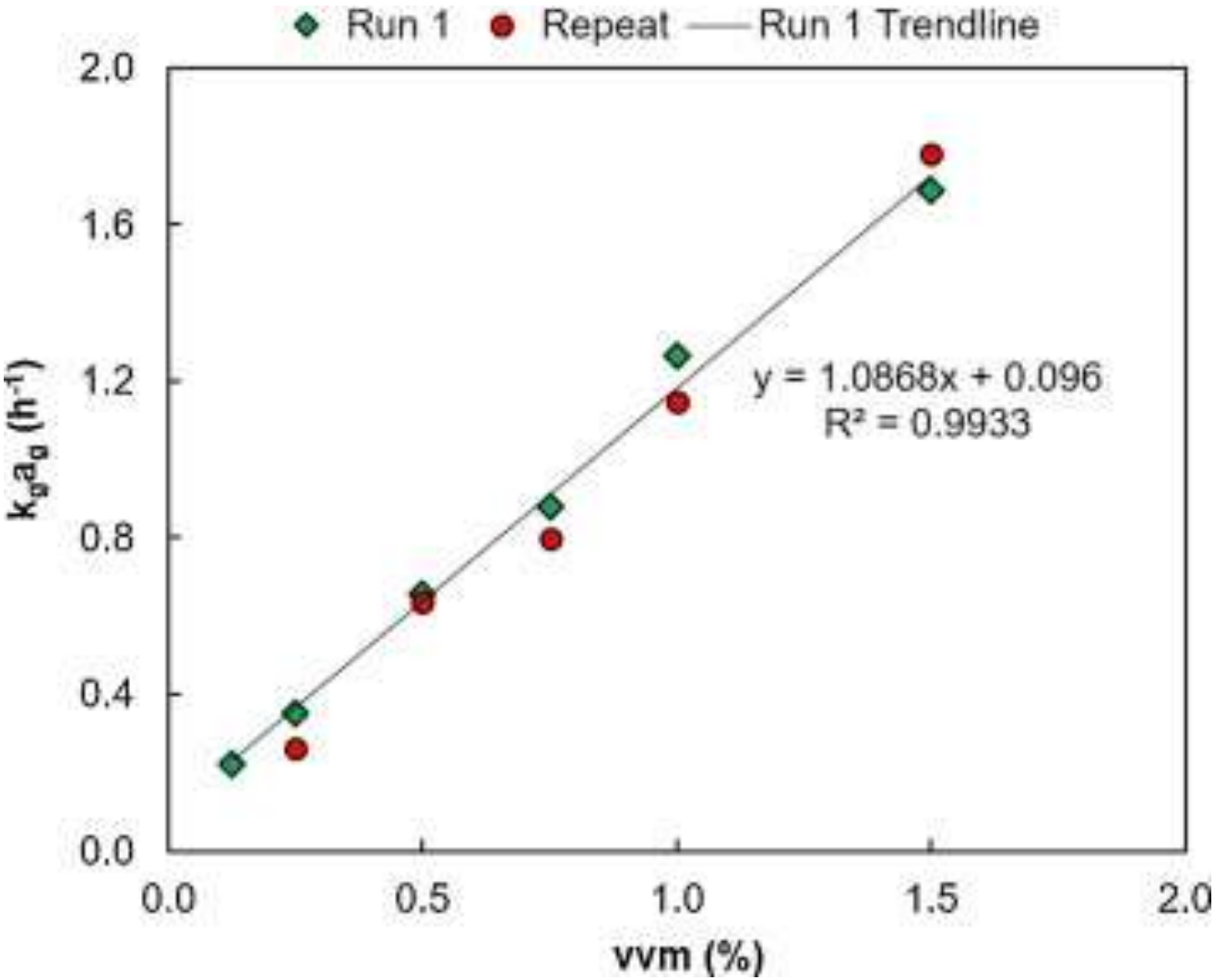

mass transfer solution. However, no differences between the initial and repeat tests were observed even though the last data point was obtained 26 days after the first. This demonstrates that the presence of biomass has a negligible influence on mass transfer efficiency and also that the procedure is repeatable. The linear relationship in Fig. 1 can be used to calculate $k_g a_g$ values at a specific vvm which, together with Eq. (9), can be used to determine the corresponding value of C_{CO_2} and also the percentage CO_2 saturation.

Continuous fermentations

The overall results of the three continuous fermentations are summarised in Table 1 in order of decreasing C_{CO_2}. Succinic acid concentrations were between 6.8 and 12.7 $g.L^{-1}$ with yields on glucose between 0.40 and 0.57 $g.g^{-1}$ and productivities between 0.3 and 1.6 $g.L^{-1}.h^{-1}$. On average, mass balance closures were 91% with a standard deviation of 3% which indicates that more glucose was consumed than was accounted for in the metabolites. This observation is similar to previous continuous fermentations with *A. succinogenes* biofilms where incomplete mass balance closures were observed on glucose [18], xylose [15] and corn stover hydrolysate [18]. In addition, the fermentation results are in agreement with previous studies on *A. succinogenes* using a complex fermentation medium containing yeast extract and no corn steep liquor [13,19]. Ethanol formation was found to increase with decreasing C_{CO_2} levels which is in agreement with [8]**,** where ethanol formation was observed at CO_2 limiting conditions. Pyruvic acid formation was observed across various C_{CO_2} levels but no distinct trend was found. Pyruvic acid production has been reported as a minor [7] and a considerable by-product [6] in glucose fermentations with *A. succinogenes* and as a more substantial by-product in continuous xylose fermentations [15].

Table 1. Summary of the data for all three fermentations (runs).

Run	CO_2 vvm (%)	C_{CO_2} (mM)	CO_2 saturation (%)	D (h^{-1})	C_{SA} ($g.L^{-1}$)	C_{AA} ($g.L^{-1}$)	C_{FA} ($g.L^{-1}$)	C_{EtOH} ($g.L^{-1}$)	C_{PYR} ($g.L^{-1}$)	C_{GLCout} ($g.L^{-1}$)	ΔC_{GLC} ($g.L^{-1}$)	Y_{GLCSA} ($g.g^{-1}$)	Y_{AASA} ($g.g^{-1}$)	Y_{AAFA} ($g.g^{-1}$)
1	6.00	15.4	67	0.124	12.2	6.4	4.9	0.34	0	1.63	21.5	0.57	1.92	0.78
	1.50	8.5	37	0.124	11.5	6.4	5.0	0.95	0	2.08	21.1	0.54	1.79	0.78
	1.00	7.6	33	0.103	11.0	6.2	4.9	0.32	0	2.97	20.1	0.54	1.76	0.79
	0.75	5.6	24	0.095	11.3	6.5	5.1	0.15	0.32	1.85	21.2	0.53	1.75	0.79
	0.50	3.9	17	0.081	11.2	6.6	5.2	0.16	0.29	1.37	21.5	0.52	1.70	0.79
	0.25	2.1	9	0.069	9.0	6.1	5.3	0.86	0.46	3.17	18.3	0.49	1.49	0.87
	0.13	1.6	7	0.055	7.4	5.7	5.6	1.12	0.76	3.09	18.1	0.41	1.30	0.98
	0.06	1.2	5	0.044	6.8	5.6	5.1	1.00	0.32	4.06	17.0	0.40	1.22	0.90
2	8.00	17.6	77	0.124	11.3	7.0	5.4	0	0	0.313	20.8	0.54	1.60	0.77
	8.00	17.5	77	0.129	12.7	7.7	5.9	0	0.24	0.28	23.1	0.55	1.66	0.77
	6.00	17.0	75	0.131	10.9	6.7	5.3	0	0	0.45	19.6	0.56	1.62	0.78
	4.00	16.0	70	0.131	10.5	6.7	5.2	0	0	0.46	19.6	0.54	1.59	0.78
	2.50	14.4	63	0.128	11.2	7.1	5.8	0	0.40	0.54	23.1	0.49	1.57	0.82
3	2.96	12.4	54	0.124	12.2	7.5	6.2	0.39	0.08	0.16	23.4	0.52	1.63	0.83
	2.50	11.7	51	0.124	11.6	7.2	6.1	0.40	0	0.59	22.9	0.51	1.63	0.85
	2.00	10.1	44	0.123	12.4	7.5	6.4	0.32	0	0.32	23.3	0.53	1.65	0.85
	1.51	8.2	36	0.123	12.3	7.5	6.4	0.39	0.16	0.3	23.3	0.53	1.63	0.84
	1.50	8.7	38	0.125	11.0	7.7	7.1	0.86	0.04	0.54	23.0	0.5	1.44	0.80

Productivity threshold

The succinic acid productivity and rate of glucose uptake remained approximately constant with decreasing C_{CO_2} down to a critical level, below which both parameters started to decrease (Fig. 2). The C_{CO_2} level at which the decrease in succinic acid productivity and substrate uptake occurred can be considered an upper C_{CO_2} threshold or *productivity threshold* ($C^{P}_{CO_2}$). In the current fermentation system, $C^{P}_{CO_2}$ is equal to 8.4 mM CO_2 which corresponds to approximately 36.8% CO_2 saturation. Since the biomass concentration is assumed to remain constant due to the imposed substrate limitation (through dilution rate adjustments), a decrease in productivity and substrate uptake suggests that either the cells are dying or the productivity per cell is decreasing, reflecting a decrease in the overall metabolic rate. It was observed that steady-states could be maintained for extended periods (greater than 48 hours) at low CO_2 flow rates which hints that the decrease in productivity is related to a decrease in metabolic activity instead of cell death. This is plausible as one would expect a persistent decrease in productivity as cells died off, thereby preventing steady-state operation which was not the case in the current study.

The observation that SA productivity is independent of C_{CO_2} above values of 8.4 mM ties in with the results of [10] where variations in the CO_2 partial pressure, hence C_{CO_2} (5.1, 10.1, 15.2, and 20.2 mM dissolved C_{CO_2}), was found to have no influence on final SA concentrations over constant batch times, although no decrease in productivity was observed at the 5.1 mM condition either. However, [12] showed that SA yield and titre were enhanced when increasing the fermentation pressure from 101.3 kPa to 140 kPa, due to the increased CO_2 partial pressure and consequently higher CO_2 saturation level in the broth. It is expected that CO_2 availability to the cell should influence SA productivity since CO_2 is essential for reductive TCA cycle flux (Fig. 3)and PEP carboxykinase activity in *A. succinogenes*. Furthermore,

Fig. 2. The rate of glucose consumption and succinic acid production as a function of the dissolved CO_2 concentration in the fermentation broth (also given as the fraction of CO_2 saturation). The vertical arrow indicates the C_{CO2} level (8.4 mM or 36.8% saturated) at which the productivity and rate of glucose uptake starts to decrease (i.e. overall metabolic rate slows) and is considered the upper CO_2 or productivity threshold ($C^{P}_{CO_2}$).

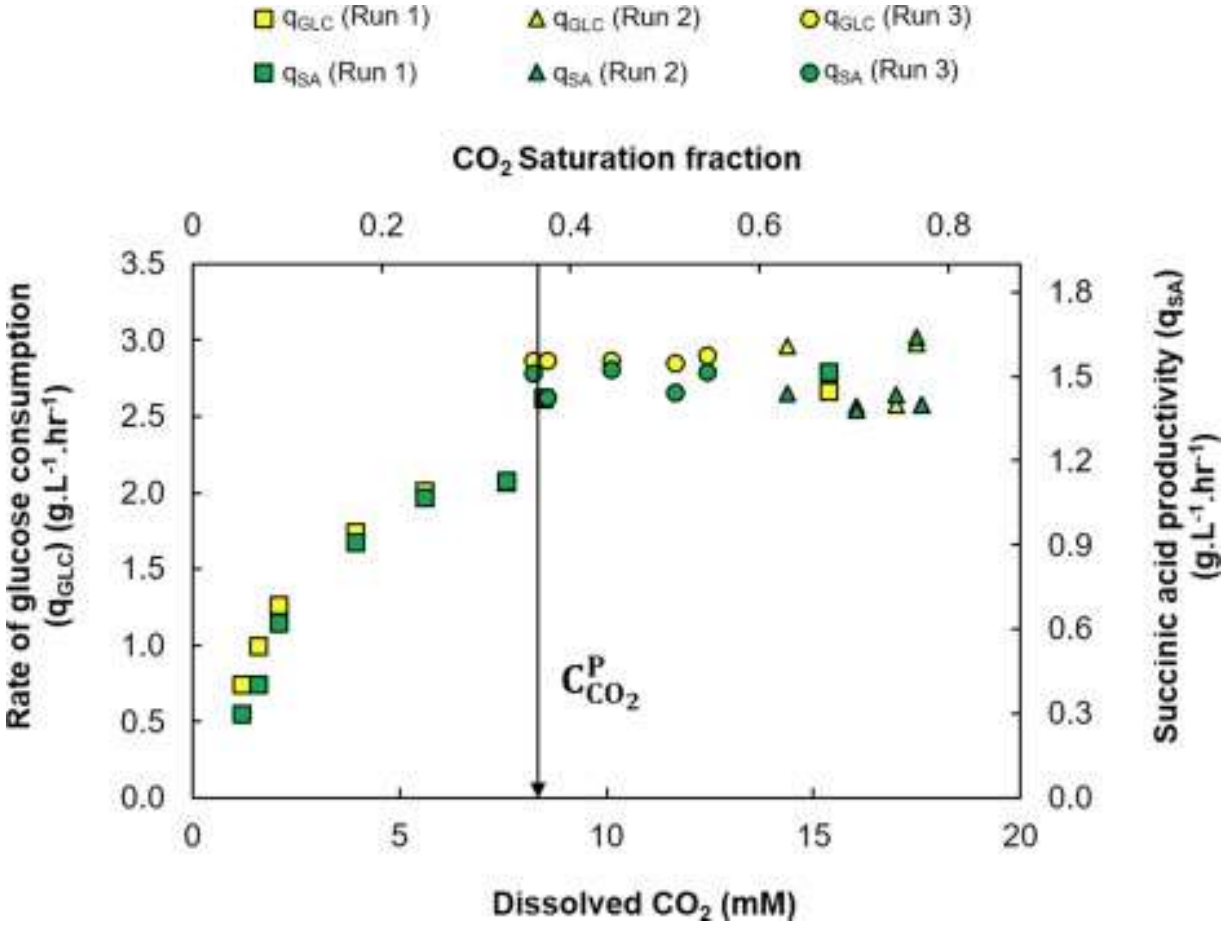

Fig. 3. Simplified central metabolic network of *A. succinogenes* showing all relevant pathways and metabolites. Adapted from [21] and [22]. AA = acetic acid; AcCoA = acetyl-CoA; EtOH = ethanol; FA = formic acid; G3P = glyceraldehyde-3-phosphate; Glc = glucose; PEP = phosphoenolpyruvic acid; Pyr = pyruvic acid; Pyr_{ex} = excreted pyruvic acid; SA = succinic acid.

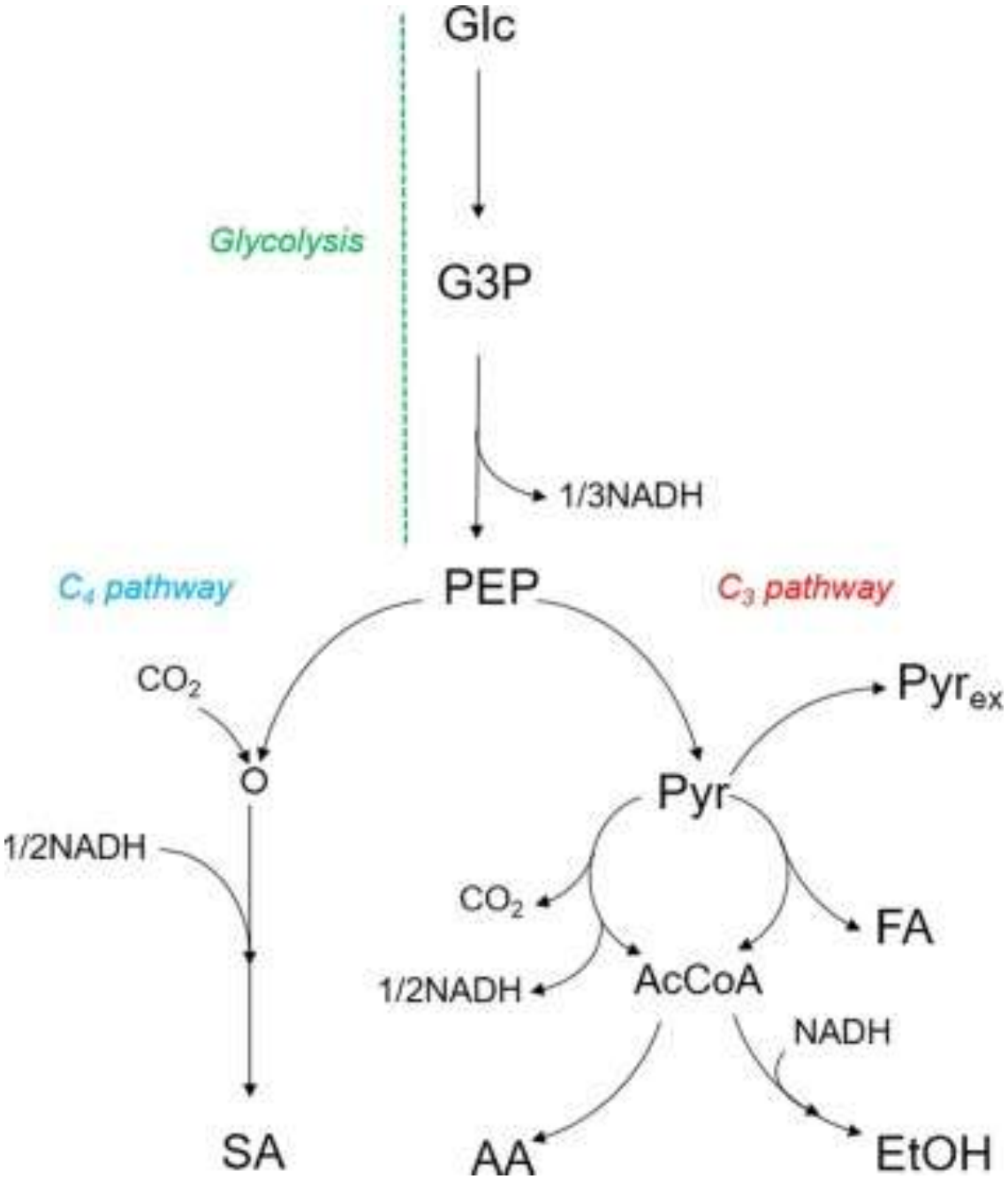

[9] showed that in fermentations of a mutant *E. coli* strain, the specific productivity and yield of SA improved substantially with increasing CO_2 fraction (i.e. partial pressure) in the gas phase. In addition, an increase in carbon flux through the pentose phosphate pathway was observed to account for the increased demand for reduced cofactors.

Yield threshold

Similar to the trend of succinic acid productivity versus C_{CO_2}, the metabolite distributions remained constant with decreasing C_{CO_2} down to a critical C_{CO_2} level (Fig.4) of 3.9 mM CO_2 (17.1% of saturation). Below this level, the concentration of succinic acid started to decrease rapidly while acetic acid and formic acid concentrations remained fairly stable. A decrease in succinic acid concentration, while by-product concentrations remain constant or decrease to a smaller degree, is indicative of a shift in carbon flux away from the C_4 pathway and towards the C_3 pathway resulting in a decrease in the yield of succinic yield (fig. 3). Therefore, the C_{CO_2} level at which this occurs can be considered a *yield threshold* and can be viewed as the lower C_{CO_2} threshold ($C^{Y}_{CO_2}$) since it occurs at a lower C_{CO_2} value to $C^{P}_{CO_2}$ (8.4 mM).

The shift in carbon flux distribution occurs at the phosphoenolpyruvic acid (PEP) node which serves as the branch point between the C_3 and C_4 pathways. The shift can be further visualised in Fig. 5 where the fraction of total carbon flux in the C_4 branch (f_4) decreases with decreasing C_{CO_2}. The fluxes through the C_3 and C_4 pathways are calculated based on the measured metabolite concentrations. Interestingly, the fraction of total carbon in the C_4 branch only starts to decrease at very low C_{CO_2} concentrations (17.1% of CO_2 saturation).

The flux shift under low C_{CO_2} values suggests that a rate-limitation at the PEP node necessitates that flux be directed to the C_3 pathway. Ethanol formation consumes two NADH molecules in *A. succinogenes* [20] and can therefore serve as a redox sink within the central

Fig. 4. The metabolite concentrations as a function of the dissolved CO_2 concentration in the broth. The distribution of metabolites remained constant down to a specific C_{CO2} level ($C^{Y}_{CO_2}$), below which SA production started to decrease.

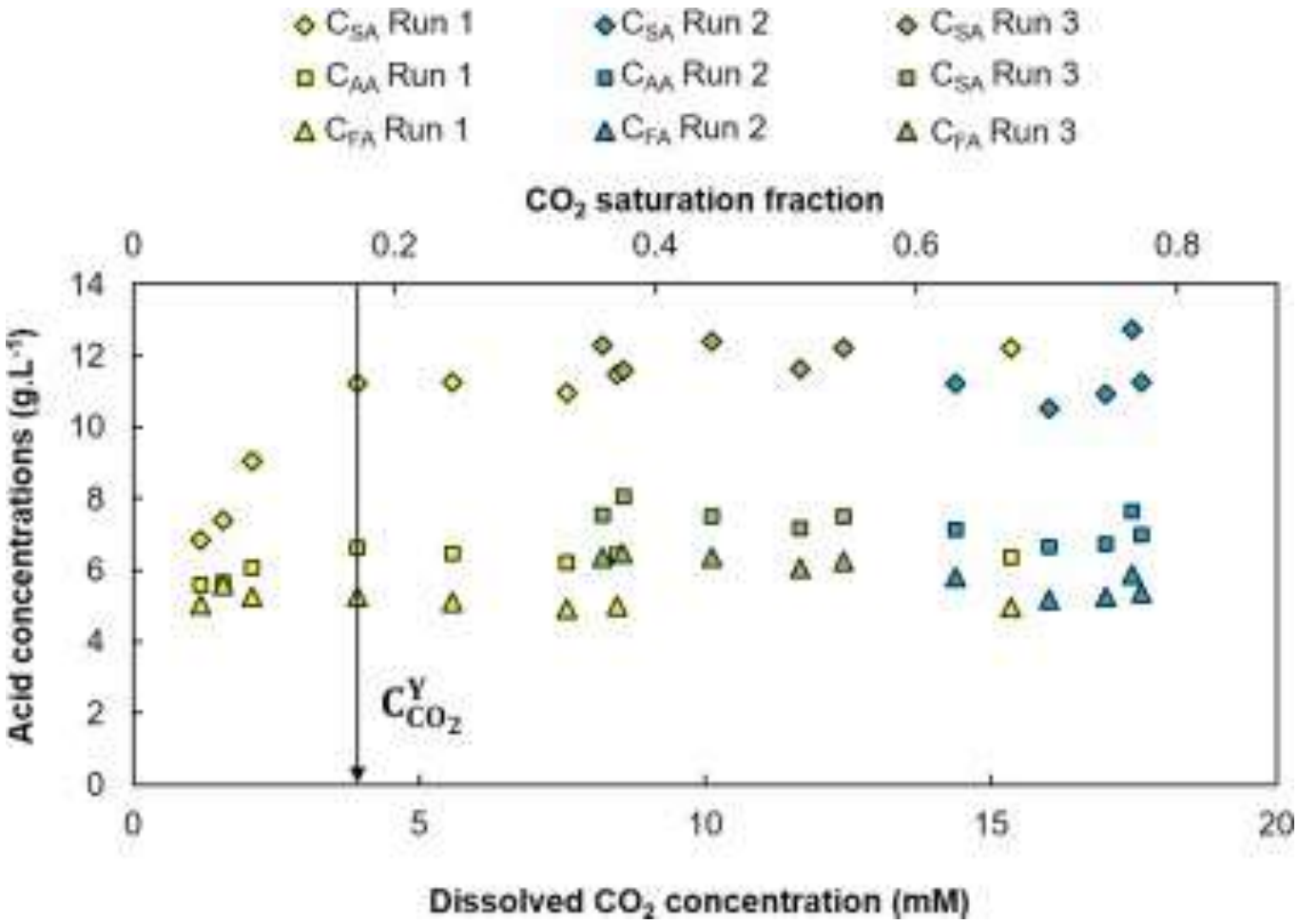

Fig. 5. The fraction of total carbon flux in the C_4 branch (f_4) as a function of the dissolved CO_2 concentration in the fermentation broth. The vertical arrow indicates the C_{CO2}CCO2 level at which a shift in carbon flux distribution is observed and is considered the lower CO_2 or yield threshold ($C^{Y}_{CO_2}$).

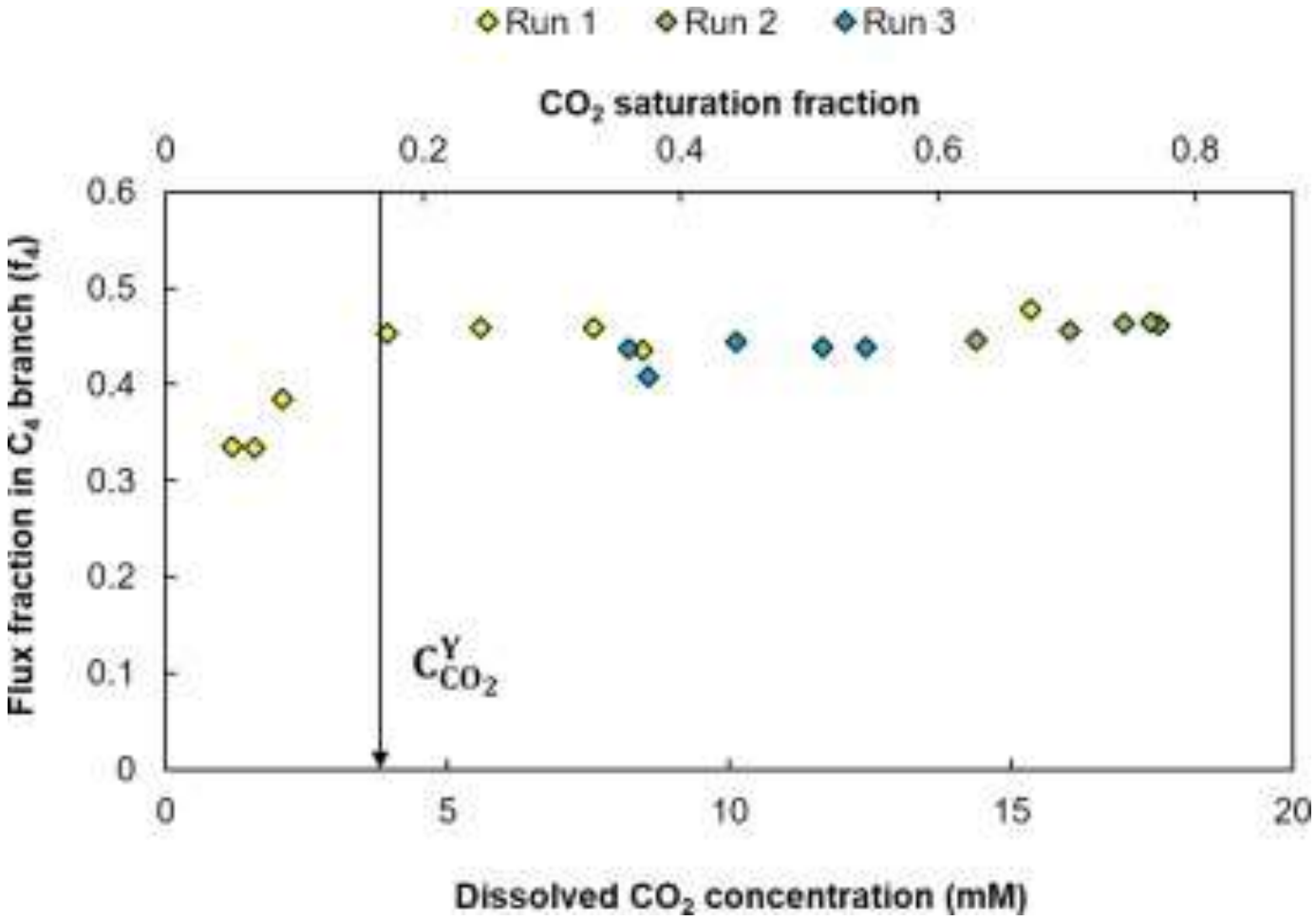

metabolism and as an alternative to the C_4 pathway. If the PEP carboxykinase reaction is rate-limited due to insufficient CO_2 availability, carbon flux to the C_3 pathway at the PEP node could increase in order to balance redox via ethanol formation. While a flux shift occurred at the PEP node, flux at the pyruvate node proceeded solely via the pyruvate formate-lyase pathway as reflected by equimolar concentrations of formic acid and acetyl-CoA (Fig. 6). If pyruvate dehydrogenase or formate dehydrogenase activity were present, the ratio of acetyl-CoA to formic acid would increase proportionately since less formic acid would be formed per mole of acetyl-CoA formed. Furthermore, the formic acid-to-acetic acid ratio remained near the equimolar value of 0.77 g g^{-1}, except during ethanol formation where the ratio increased because a fraction of acetyl-CoA was converted to ethanol instead of acetic acid.

The decrease in C_{CO_2} in the broth directly affects the rate of CO_2 uptake once $C^{P}_{CO_2}$ is reached. Below $C^{P}_{CO_2}$, the rate of PEP carboxylation (and succinic acid formation) decreases. The results suggest that glucose uptake in the region between the two thresholds (i.e. $C^{Y}_{CO_2} < C_{CO_2} < C^{P}_{CO_2}$) decreases in proportion to succinic acid flux, while the distribution of metabolites remains the same as when $C_{CO_2} > C^{P}_{CO_2}$. This implies that the cellular rate of ATP generation also decreases. Therefore, less energy is available to the organism for maintenance processes yet the organism remains viable as seen by the prolonged operation under these conditions ($C^{Y}_{CO_2} < C_{CO_2} < C^{P}_{CO_2}$).

A further decrease in C_{CO_2} leads to the condition where $C_{CO_2} < C^{Y}_{CO_2}$. Once the system enters this regime, a shift in metabolic flux distribution occurs where ethanol begins to form while carbon flux to succinic acid decreases. The low rate of CO_2 uptake leads directly to the reduction in both succinic acid flux and PEP carboxylation. The question then arises why acetyl-CoA flux increases under this condition. It is evident that the redox balance

Fig. 6. A parity plot of formic acid and acetyl-CoA. The solid diagonal line represents equimolar concentrations; data points lying on this line reflect exclusive pyruvate formate-lyase activity.

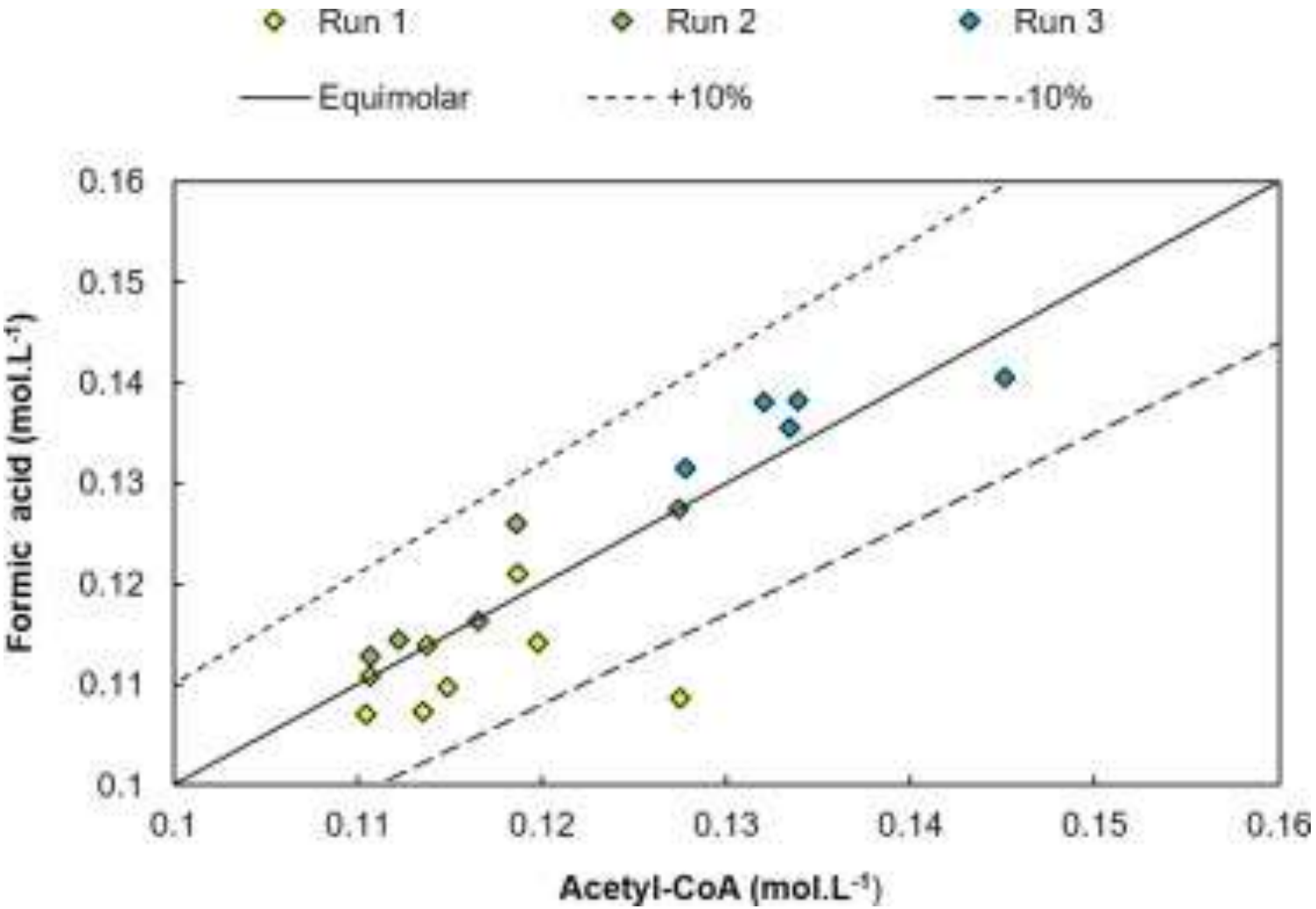

necessitates ethanol formation in order to consume excess NADH because succinic acid flux, hence flux through the reductive branch of the TCA cycle, decreases. However, the energy (i.e. ATP) implications of the shift are not obvious. Assuming that 2/3 mole ATP is produced in converting fumaric acid to succinic acid [20], the yield of ATP on glucose consumed (Y_{SATP}) can be calculated via a simple metabolic flux model where a redox balance is specified with no dehydrogenase activity (i.e. all pyruvate is converted by pyruvate formate-lyase). The theoretical results are shown in Fig. 7 where both the ethanol (Y_{SE}) and ATP (Y_{SATP}) yield on glucose are given as a function of the fraction of PEP converted to succinic acid (f_{SA}). It is clear that no gain in ATP is achieved with a decrease in f_{SA}. Therefore, the increase in acetyl-CoA flux does not provide any energy advantages and appears to be merely an overflow caused by the primary need to balance redox, where glucose uptake does not decrease in proportion to succinic acid flux. Consequently, the organism experiences a further decrease in the cellular rate of ATP generation. Despite this, the results suggest that cells are still viable under this condition as protracted steady-states were observed.

4. Conclusions

CO_2 is an important co-substrate in succinic acid production by *A. succinogenes*. To ensure efficient succinic acid production, the availability of CO_2 to the cells needs to be maximised. In this study it is demonstrated that CO_2 availability, as dissolved CO_2 concentration (C_{CO_2}) and percentage saturation of the fermentation broth, has two main thresholds when operating under continuous conditions. The first, or upper threshold, occurs at a C_{CO_2} of 8.4 mM (36.8% saturation) and a gradual decrease in SA productivity and glucose uptake occurs as C_{CO_2} is decreased below this threshold. As C_{CO_2} is decreased further, a second, or lower, threshold occurs at 3.9 mM C_{CO_2} (17% saturation) below which SA productivity decreases further together with a shift in carbon flux away from the C_4 pathway (succinic acid route) towards the C_3 pathway (by-product route). In addition to the usual by-products (i.e. acetic- and formic acid), ethanol formation was observed below the second threshold, likely as a means to balance redox. The CO_2 thresholds occur at low values relative to full saturation, which is advantageous from an industrial processing perspective as it implies that the bulk liquid does not need to be maintained near CO_2 saturation at all times. Instead, there can be some flexibility in the control of CO_2 which may allow for reduced sparging and compression needs (i.e. lower CO_2 pressure) thereby reducing operating expenses. Therefore, the results are useful for future design and optimisation of CO_2 mass transfer systems in succinic acid fermentations with *A. succinogenes*.

Nomenclature

C_{AA}	acetic acid concentration	$g.L^{-1}$
$C_{CO_2}^{eq}$	CO_2 concentration at equilibrium	$mol.L^{-1}$
C_{CO_2}	dissolved CO_2 concentration in broth	$mol.L^{-1}$
$C_{CO_2}^{*}$	dissolved CO_2 concentration at saturation	$mol.L^{-1}$
$C_{CO_2}^{P}$	dissolved CO_2 concentration at productivity threshold	$mmol.L^{-1}$
$C_{CO_2}^{Y}$	dissolved CO_2 concentration at yield threshold	$mmol.L^{-1}$
$C_{H^+}^{feed}$	proton concentration in feed	$mol.L^{-1}$
C_{H^+}	proton concentration in broth	$mol.L^{-1}$
$C_{H^+}^{eq}$	hydronium ion concentration at equilibrium	$mol.L^{-1}$
$C_{H_2CO_3}^{eq}$	H_2CO_3 concentration at equilibrium	$mol.L^{-1}$
$C_{HCO_3^-}^{eq}$	HCO_3^- concentration at equilibrium	$mol.L^{-1}$
C_{OH}	sodium hydroxide concentration	$mol.L^{-1}$
C_{SA}	succinic acid concentration	$g.L^{-1}$
f_4	fraction of total carbon flux in the C_4 pathway	
f_{SA}	fraction of phosphoenolpyruvic acid converted to succinic acid	
H_0	Henry's constant in pure solvent	$kPa.L.mol^{-1}$
K_1	equilibrium constant – carbonic acid formation	$mol.L^{-1}$
K_2	equilibrium constant – bicarbonate formation	$mol.L^{-1}$
K_3	equilibrium constant – carbonate formation	$mol.L^{-1}$
K_4	equilibrium constant	$mol.L^{-1}$
$k_g a_g$	gas-based mass transfer coefficient	h^{-1}
$P_{CO_2}^{*}$	CO_2 partial pressure	kPa
Q	overall volumetric flow rate	$mL.min^{-1}$
Q_D	sodium hydroxide flow rate	$mL.min^{-1}$
Q_{feed}	feed flow rate	$mL.min^{-1}$
q_{Glc}	glucose consumption rate	$g.L^{-1}h^{-1}$
q_{SA}	succinic acid productivity	$g.L^{-1}h^{-1}$
r_{CO_2}	rate of CO_2 transfer	$mol.L^{-1}.h^{-1}$
V	reactor volume	mL

References

[1] J.J. Bozell, G.R. Petersen, Technology development for the production of biobased products from biorefinery carbohydrates—the US Department of Energy's "Top 10" revisited, Green Chem. 12 (2010) 539. doi:10.1039/b922014c.

[2] M. Patel, M. Cranck, V. Dornburg, B. Hermann, L. Roes, B. Husing, The BREW project - Medium and Long-term Opportunities and Risks of the Biotechnological Production of Bulk Chemicals from Renewable Resources, 2006.

[3] H. Song, S.Y. Lee, Production of succinic acid by bacterial fermentation, Enzyme Microb. Technol. 39 (2006) 352–361. doi:10.1016/j.enzmictec.2005.11.043.

[4] I. Bechthold, K. Bretz, S. Kabasci, R. Kopitzky, A. Springer, Succinic Acid: A new platform chemical for biobased polymers from renewable resources, Chem. Eng. Technol. 31 (2008) 647–654. doi:10.1002/ceat.200800063.

[5] J.J. Beauprez, M. De Mey, W.K. Soetaert, Microbial succinic acid production: Natural versus metabolic engineered producers, Process Biochem. 45 (2010) 1103–1114. doi:10.1016/j.procbio.2010.03.035.

[6] S.K.C. Lin, C. Du, A. Koutinas, R. Wang, C. Webb, Substrate and product inhibition kinetics in succinic acid production by *Actinobacillus succinogenes*, Biochem. Eng. J. 41 (2008) 128–135. doi:10.1016/j.bej.2008.03.013.

[7] M. Guettler, D. Rumler, M. Jain, *Actinobacillus succinogenes* sp. nov., a novel succinic-acid-producing strain from the bovine rumen, Int. J. Syst. Bacteriol. 49 (1999) 207–216. http://ijs.sgmjournals.org/content/49/1/207.short (accessed December 9, 2012).

[8] M.J. Van der Werf, M. V Guettler, M.K. Jain, J.G. Zeikus, Environmental and

physiological factors affecting the succinate product ratio during carbohydrate fermentation by *Actinobacillus* sp. 130Z, Arch. Microbiol. 167 (1997) 332–42. http://www.ncbi.nlm.nih.gov/pubmed/9148774.

[9] S. Lu, M. a Eiteman, E. Altman, Effect of CO_2 on succinate production in dual-phase *Escherichia coli* fermentations., J. Biotechnol. 143 (2009) 213–23. doi:10.1016/j.jbiotec.2009.07.012.

[10] W. Zou, L.-W. Zhu, H.-M. Li, Y.-J. Tang, Significance of CO_2 donor on the production of succinic acid by *Actinobacillus succinogenes* ATCC 55618, Microb. Cell Fact. 10 (2011) 87. doi:10.1186/1475-2859-10-87.

[11] Y. Xi, K. Chen, J. Li, X. Fang, X. Zheng, S. Sui, et al., Optimization of culture conditions in CO2 fixation for succinic acid production using *Actinobacillus succinogenes*, J. Ind. Microbiol. Biotechnol. 38 (2011) 1605–12. doi:10.1007/s10295-011-0952-5.

[12] I.B. Gunnarsson, M. Alvarado-Morales, I. Angelidaki, Utilization of CO_2 fixating bacterium *Actinobacillus succinogenes* 130Z for simultaneous biogas upgrading and biosuccinic acid production, Environ. Sci. Technol. 48 (2014) 12464–8. doi:10.1021/es504000h.

[13] R.I. Corona-González, A. Bories, V. González-Álvarez, C. Pelayo-Ortiz, Kinetic study of succinic acid production by *Actinobacillus succinogenes* ZT-130, Process Biochem. 43 (2008) 1047–1053. doi:10.1016/j.procbio.2008.05.011.

[14] M.F.A. Bradfield, W. Nicol, Continuous succinic acid production by *Actinobacillus succinogenes* in a biofilm reactor: Steady-state metabolic flux variation, Biochem. Eng. J. 85 (2014) 1–7. doi:10.1016/j.bej.2014.01.009.

[15] M.F.A. Bradfield, W. Nicol, Continuous succinic acid production from xylose by *Actinobacillus succinogenes*, Bioprocess Biosyst. Eng. 39 (2016) 233–244. doi:10.1007/s00449-015-1507-3.

[16] C. Van Heerden, W. Nicol, Continuous succinic acid fermentation by *Actinobacillus succinogenes*, Biochem. Eng. J. 73 (2013) 5–11. doi:10.1016/j.bej.2013.01.015.

[17] H.G. Brink, W. Nicol, Succinic acid production with *Actinobacillus succinogenes*: rate and yield analysis of chemostat and biofilm cultures., Microb. Cell Fact. 13 (2014) 111. doi:10.1186/s12934-014-0111-6.

[18] M.F.A. Bradfield, A. Mohagheghi, D. Salvachúa, H. Smith, B.A. Black, N. Dowe, et al., Continuous succinic acid production by *Actinobacillus succinogenes* on xylose-enriched hydrolysate, Biotechnol. Biofuels. 8 (2015) 181. doi:10.1186/s13068-015-0363-3.

[19] R.I. Corona-Gonzalez, A. Bories, V. González-Alvarez, R. Snell-Castro, G. Toriz-González, C. Pelayo-Ortiz, Succinic acid production with *Actinobacillus succinogenes* ZT-130 in the presence of succinic acid, Curr. Microbiol. 60 (2010) 71–7. doi:10.1007/s00284-009-9504-x.

[20] J.B. McKinlay, M. Laivenieks, B.D. Schindler, A. a McKinlay, S. Siddaramappa, J.F. Challacombe, et al., A genomic perspective on the potential of *Actinobacillus succinogenes* for industrial succinate production., BMC Genomics. 11 (2010) 680. doi:10.1186/1471-2164-11-680.